

Sepsis induces an increase in thick ascending limb Cox-2 that is TLR4 dependent

Tarek M. El-Achkar, Zoya Plotkin, Branislav Marcic, and Pierre C. Dagher

Indiana Center for Biological Microscopy, Department of Medicine, Division of Nephrology, Indiana University, Indianapolis, Indiana

Submitted 10 May 2007; accepted in final form 12 July 2007

El-Achkar TM, Plotkin Z, Marcic B, Dagher PC. Sepsis induces an increase in thick ascending limb Cox-2 that is TLR4 dependent. *Am J Physiol Renal Physiol* 293: F1187–F1196, 2007. First published July 18, 2007; doi:10.1152/ajprenal.00217.2007.—Cyclooxygenase-2 (Cox-2) is an inducible enzyme responsible for the formation of inflammatory prostanoids such as prostaglandins and thromboxane. Its role in the pathophysiology of inflammatory states like sepsis is increasingly recognized. Recently, we demonstrated that sepsis up-regulates the endotoxin receptor Toll-like receptor 4 (TLR4) in rat kidney. Because Cox-2 is one of the downstream products of TLR4 activation, we hypothesized that sepsis-induced changes in renal Cox-2 expression are TLR4 dependent. Indeed, we show that in Sprague-Dawley rats, cecal ligation and puncture (a sepsis model) increases Cox-2 expression in cortical and medullary thick ascending loops (cTAL and mTAL, respectively) as well as inner medullary collecting ducts. These are all sites of increased TLR4 expression during sepsis. To determine the actual dependence on TLR4, we measured Cox-2 expression in wild-type and mutant mice which harbor a *TLR4* gene deletion (*TLR4*^{-/-}). In wild-type mice, sepsis increased Cox-2 expression in proximal tubules, cTAL, and mTAL. In contrast, septic *TLR4*^{-/-} mice showed no significant increase in cTAL or mTAL Cox-2 expression. Furthermore, renin was absent from juxtaglomerular cells of *TLR4*^{-/-} mice. We conclude that the dependence of sepsis-induced renal Cox-2 expression on TLR4 is tubule specific. The TLR4-dependent Cox-2 expression is mostly restricted to cortical and medullary thick ascending loops of Henle that characteristically express and secrete Tamm-Horsfall protein.

Toll-like receptors; renin; Tamm-Horsfall protein; macula densa; cyclooxygenase

TOLL-LIKE RECEPTORS (TLRs) mediate the interaction between pathogens and host defenses (2). Their location on cells of the immune system allow them to recognize and interact with specific pathogen-associated molecular patterns and thereby initiate a cascade of signaling events that includes an early inflammatory response (1). In addition, TLRs can also be stimulated by endogenous ligands and thus play a role in various processes like immune-mediated diseases, ischemia, and atherogenesis (30). TLRs are also located on parenchymal epithelial and endothelial cells in various organs. These organ-specific TLRs may be involved in modulating responses to systemic or local stimuli.

Together with other investigators, we recently demonstrated the presence of TLRs in the kidney (10). The expression of these receptors is altered by various forms of injury like sepsis,

ischemia, and cyclosporine toxicity (9). Data also exist that support a functional role for TLRs in ischemic renal injury (22). In contrast, the role of renal TLRs in sepsis remains more controversial (6, 7, 9, 41). This stems in part from the complexity of sepsis-induced renal injury where multiple systemic and local factors are involved. Furthermore, the multitude of models utilized to induce animal sepsis has resulted in conflicting data, thus hindering our understanding of the pathophysiology of this elusive disease (29).

In cells of the innate immune system, one of the downstream products of TLR signaling is cyclooxygenase-2 (Cox-2) (1). This inducible isoform of the cyclooxygenase enzyme catalyzes the formation of prostaglandins, which can mediate a significant inflammatory response (14). In the kidney, Cox-2 is constitutively expressed but can also be upregulated in response to various stimuli (5, 12, 15, 16, 18, 34, 38–40). It is thought to impact many processes such as local hemodynamics (24), urinary concentration (12, 26), and renin production (32). In the rat kidney, Cox-2 is expressed in the cortex, outer medulla, and inner medulla. However, some variability does exist between reports as to the specific renal cell types expressing Cox-2 in the rat (5, 18). There is even more inconsistency regarding the sites of Cox-2 expression in the mouse kidney (5, 35).

Systemic Cox-2 is increasingly recognized as an important player in sepsis-induced inflammation. In fact, Cox-2-deficient mice are protected from sepsis-induced inflammation and death (8). However, data on the specific effects of sepsis on renal Cox-2 are very limited and rely primarily on the lipopolysaccharide (LPS) injection model (18, 40). This sepsis model is increasingly criticized because it results in a greatly exaggerated cytokine profile that might not reflect adequately true human sepsis (29).

In this study, we tested the hypothesis that sepsis alters renal Cox-2 expression in rat and mouse kidneys in a cell-specific manner. We also investigated whether these changes in Cox-2 are TLR4 dependent. Cox-2 protein localization and quantitation were done with immunofluorescence microscopy. Sepsis was induced with cecal ligation and puncture (CLP), a model considered more relevant to human sepsis. In both rats and wild-type mice, sepsis induced robust upregulation of Cox-2 expression in various tubular segments. In TLR4 knockout mice, sepsis-induced Cox-2 upregulation was significantly diminished in Tamm-Horsfall protein (THP)-expressing medullary and cortical thick ascending limbs (mTAL and cTAL, respectively).

In addition, TLR4 knockout mice showed reduced renin expression in juxtaglomerular cells. Thus renal TLR4 and

Address for reprint requests and other correspondence: P. C. Dagher, Dept. of Medicine, Div. of Nephrology, 950 W. Walnut St., R2-202A, Indianapolis, IN 46202 (e-mail: pdaghe2@iupui.edu tarek.elachkar@va.gov).

Present address of T. M. El-Achkar; Dept. of Medicine, Div. of Nephrology, Saint Louis University, and the John Cochran Veterans Affairs Medical Center, Saint Louis, MO.

The costs of publication of this article were defrayed in part by the payment of page charges. The article must therefore be hereby marked “advertisement” in accordance with 18 U.S.C. Section 1734 solely to indicate this fact.

Cox-2 are potentially important players in the renal response to sepsis.

METHODS

Animal Surgery

All animal experimentation was approved by the Indiana University Animal Care Committee and conducted in conformity with the *Guiding Principles for Research Involving Animals and Human Beings*.

CLP is the preferred model for animal sepsis (17, 37). It results in a cytokine profile similar to that seen in human sepsis. It lacks the exaggerated TNF- α levels observed in the LPS injection models (29). In brief, under halothane anesthesia, the cecum of Sprague-Dawley rats (200–250 mg body wt, Harlan, Indianapolis, IN) is ligated and punctured twice with an 18-G needle. The procedure is performed on a homeothermic pad with monitoring of O₂ saturation and blood pressure. The animal is allowed to recover, and blood is collected at baseline and 24-h intervals thereafter. Surviving animals are killed at 24 h after CLP. We also performed CLP on wild-type background C57BL/10ScSNJ (*TLR4*^{+/+}) and C57BL/10ScSNJ mutant mice with *TLR4* gene deletion (*TLR4*^{-/-}) both from Jackson Laboratory. In mice, we utilized a 25-G needle to puncture the cecum. The procedure was otherwise identical to that done on rats.

In our hands, this model is characterized by a 50% reduction in glomerular filtration rate (GFR) that occurs between 24 and 48 h, with some recovery in the surviving rats. The histological changes 24 h after CLP are minimal and consist of vacuolization of tubular cells and very patchy architectural disruption. Very few casts were observed, and white blood cell infiltration (esterase reaction) averaged 1–2/field. Apoptosis in tubular cells increased up to 5% (TdT-mediated dUTP nick-end-labeling stain) compared with <1% in sham. These changes are similar to those reported by us and others previously (23).

Tissue Harvesting and Staining

After harvesting, kidneys were cut into small segments and fixed in 4% paraformaldehyde overnight. They were then preserved for 3–5 days in 30% sucrose before 10- μ m cryosections were obtained. Alternatively, kidneys were perfusion fixed in situ with 100 ml 4% paraformaldehyde, and 100- μ m sections were obtained 24 h later with a vibratome. Cryosections were mostly used for renin immunostaining, whereas vibratome sections were used for Cox-2 staining where image volume stacks were also collected. The protocols for immunostaining cryosections and vibratome sections were as we reported previously in detail (19, 21, 28).

The primary antibodies for Cox-2 utilized in our study have been used and validated in previous publications (5, 27). We used the following antibodies from Santa Cruz Biotechnology: goat polyclonal IgG primary for Cox-2 (C-20; catalog no. sc-1745) when staining rat tissue; goat polyclonal IgG primary for Cox-2 (M-19; catalog no. sc-1747) when staining mice tissue; and goat polyclonal IgG primary for renin (E-17; catalog no. sc-27318). For THP, we used a rabbit polyclonal IgG (catalog no. 8595=0004, Biogenesis). The following conjugated secondary antibodies were used: Alexa Fluor 555 donkey anti-rabbit IgG, Alexa Fluor 647 chicken anti-goat IgG (both from Molecular Probes), or Cy5 donkey anti-goat IgG (Jackson ImmunoResearch). Brush borders were stained with FITC-phalloidin, and nuclei were stained with DAPI. Negative controls were obtained by incubating tissues from sham and CLP animals with secondary antibodies in the absence of primary antibodies.

Confocal Microscopy

All images were collected using $\times 40$ magnification from fixed tissues with a Zeiss LSM 510 confocal microscope or a Bio-Rad

MRC1024 laser-scanning confocal microscope available at the Indiana Center for Biological Microscopy. Images were analyzed with Zeiss LSM software and MetaMorph (Universal Imaging) (20).

Fluorescence-Based Operational Definitions of Kidney Layers and Structures

We used the following fluorescence-based operational definitions to identify the traditional kidney layers (Fig. 1). The cortex was defined as any area containing glomeruli. In addition, proximal tubules (P in figure; FITC-phalloidin staining), THP-positive cTAL and THP-negative tubules (T-) were also identified in the cortex. T- structures represent either distal tubules or collecting ducts (CD). The outer stripe of the outer medulla (OSOM) is the area adjacent to the cortex that lacks glomeruli. It also contains proximal tubules, THP-positive

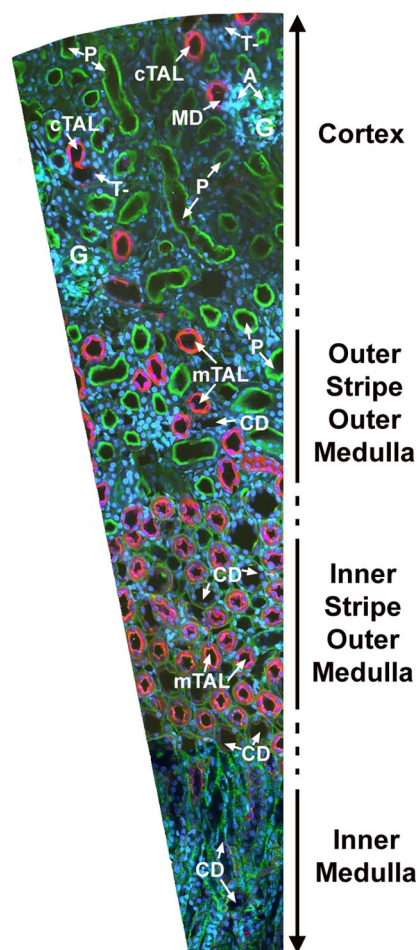


Fig. 1. Immunofluorescence landmarks of kidney layers. Shown are immunofluorescence landmarks in a rat kidney section used to identify the traditional layers. It is composed of multiple fields pasted in way to convey the real layout of a slice of kidney, extending from the cortex to the inner medulla. The dimensions are scaled up for clarity. Tamm-Horsfall protein (THP) is shown in red. Bright green represents FITC-phalloidin, which stains predominantly proximal tubular (P) brush borders but also other actin-rich structures. Darker green is tubular autofluorescence. Blue is DAPI nuclear stain. The cortex stains predominantly for glomeruli (G), P, cortical thick ascending limbs (cTAL; THP-positive), and THP-negative tubules [T-; representing distal tubules or collecting ducts (CD)]. A macula densa (MD) is shown adjacent to an afferent arteriole. Afferent and efferent arterioles are labeled A. The medulla lacks glomeruli. The outer stripe of outer medulla stains for P, medullary thick ascending limbs (mTAL; THP-positive), and T- tubules that represent primarily CD. The inner stripe of the outer medulla lacks P and stains mostly for mTAL and CD. The inner medulla, characterized by a complete absence of THP staining, has CD and thin descending limbs and TAL (not labeled).

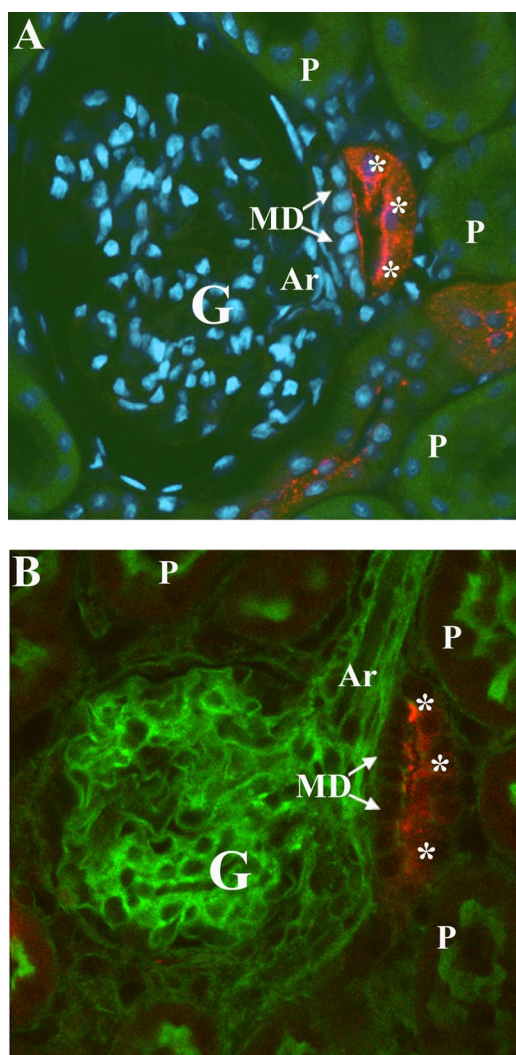


Fig. 2. Immunofluorescence staining of the MD. The MD can be easily identified by staining for THP (red). In *A*, nuclei were stained blue with DAPI. MD cells have large nuclei and completely lack THP. In contrast, opposing non-MD cells in the same cross-sectional tubular plane have intense THP staining (asterisks). MD cells are identified usually next to a glomerulus (G) and afferent arteriole (Ar). Proximal tubules (P) have dark green autofluorescence. In *B*, the MD is still recognizable despite the absence of DAPI nuclear staining. Instead, glomerular and arteriolar actin cytoskeleton are highlighted with bright green FITC-phalloidin. Proximal tubules also show FITC staining of the apical brush border. The MD cells are recognized by their large size and complete absence of THP staining in contrast to the equiplanar tubular cells (asterisks).

mTAL, and THP-negative early CD. The inner stripe of the outer medulla (ISOM) lacks proximal tubules. It contains mTAL and CD. The inner medulla lacks any THP staining. CD are the largest tubular structures identified in the inner medulla.

In Fig. 2, we show the fluorescence fingerprint of a macula densa (MD). It is invariably adjacent to a glomerulus, and the MD cells per se always lack THP staining. In contrast, the equiplanar tubular cells opposite MD cells have THP staining. This gives a crescent-shaped THP staining pattern in the cross section of the tubule at the level of the MD. Occasionally, afferent arterioles can be easily identified under the MD cells.

Quantitative Analysis

Quantitation of Cox-2 signal intensities was done using MetaMorph, version 5.0. At least eight representative fields in sham and

CLP-operated rats were analyzed using 6–10 tubules in each field. Tubules were randomly chosen, and their total tubular fluorescence intensities were averaged by the software. Furthermore, the average intensity from the negative control image was calculated and subtracted from each reading to adjust for background. In the case of the inner medulla, we also sampled equal surface areas in between CD (formed mostly by vascular structures, interstitial cells, or thin limbs) from sham and CLP-operated animals and measured average fluorescence intensities. Statistical analysis was done using a two-tailed unpaired *t*-test and 0.05 significance level. Since Cox-2 in the rat cTAL was mostly expressed in discrete cells, we counted the number of Cox-2 intensely stained cells present within the total number of cTAL pixels. The measurements are presented as number of intense cells/ 10^4 TAL pixels, knowing that one TAL tubule harbors, on average, 10^4 pixels in fields collected using our method.

Three-Dimensional Reconstruction and Volume Rendering of the MD

Stacks of Z-planes were collected at 0.4- μ m intervals. Three-dimensional (3D) volume rendering was done using Voxx, a voxel-based 3D imaging software available from the Indiana Center for

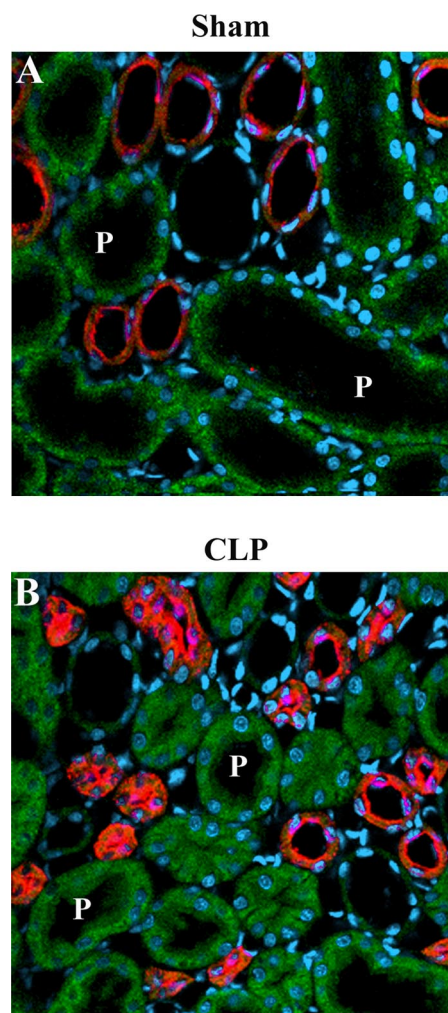


Fig. 3. Immunofluorescence staining of THP in sham and cecal ligation and puncture (CLP) rats. Shown are representative sections from the outer medulla of sham rats (*A*) and 24 h after CLP (*B*). THP is shown in red and stains the mTAL segments. Proximal tubules (P) have green autofluorescence. Nuclei are stained blue with DAPI. Note the increase in red THP fluorescence after CLP.

Biological Microscopy. A video was produced in addition to snapshot images representing views of the 3D MD from different angles.

RESULTS

Sepsis Increases THP Expression in Rat TAL

THP is a frequently used marker for cTAL and mTAL segments. However, recent data suggest possible functional roles of THP in the pathophysiology of many diseases like urinary infections, sepsis, and ischemia. We therefore examined whether THP expression in the kidney is altered by systemic sepsis. In sham-operated rats, THP staining in outer medullary mTAL segments was thin and linear and restricted to the cellular and apical regions of the tubules (Fig. 3A). After CLP, THP staining intensified and frequently extended into the mTAL lumen (Fig. 3B). We have previously reported a remarkable lack of cast formation by hematoxylin and eosin in the CLP model of sepsis (10). Therefore, this increase in THP in TAL lumens does not seem to be involved in cast formation. These changes in THP with sepsis were most prominent in the outer medulla but were also occasionally noticeable in the cortex.

Changes in Rat Renal Cox-2 Expression With Sepsis

Cortex: sepsis increases Cox-2 expression in THP-positive cTAL. In sham rats, Cox-2 expression in the cortex was minimal with occasional cells in THP-positive cTAL showing faint staining (Fig. 4, A and C). The average number of Cox-2-expressing cTAL cells under sham condition was 1.7 cells/10⁴ TAL pixels (1 TAL tubule harbors 10⁴ pixels on average in fields collected under our methods). After CLP, the number of Cox-2-positive cells in cTAL increased significantly to 3.7 cells/10⁴ TAL pixels ($P < 0.05$ compared with sham). The staining was very intense and easily identifiable in discrete cells along cTAL tubules (Fig. 4, B and D). Note that these

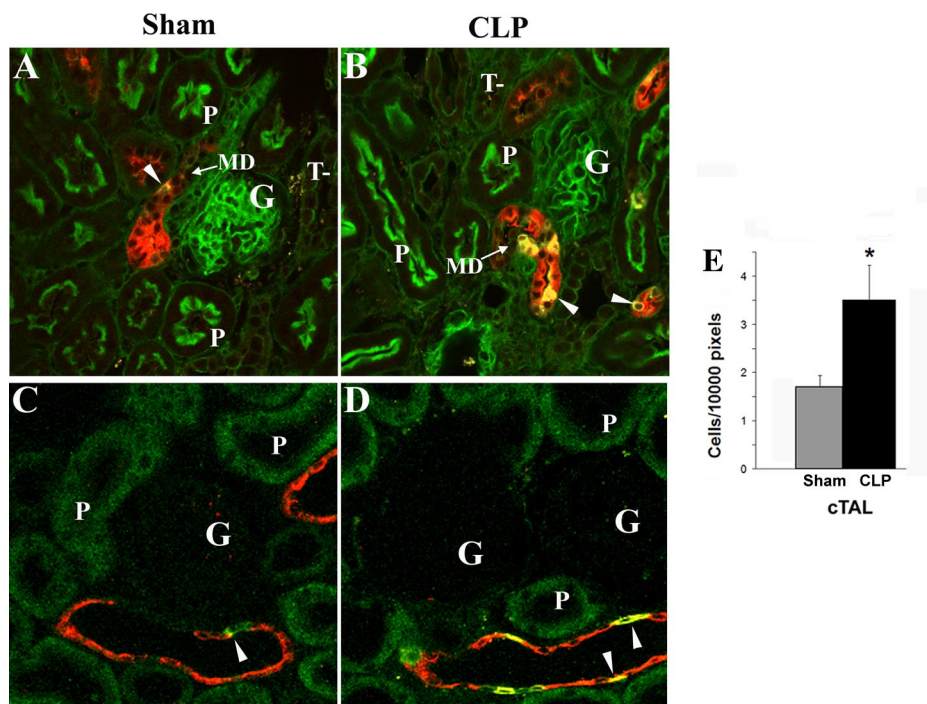
Cox-2-expressing cells had less THP staining than neighboring cell in the same tubule. Cox-2 staining was minimal in proximal and T- tubules under both sham and CLP conditions.

MD: sepsis increases Cox-2 expression in central and peripheral MD cells. In juxtaglomerular areas, MD cells, typically recognized by their columnar shape and large nuclei, show no THP staining (Figs. 2 and 5). There is controversy regarding Cox-2 expression by MD cells (5, 18). This controversy probably stems from the presence of two populations of MD cells (Fig. 5): the peripheral cells (labeled numerically) and the central cells (labeled alphabetically with hand-drawn contours). The actual functional differences between these two cell populations are not well understood.

Both peripheral and central MD cells exhibit Cox-2 staining under CLP conditions. The staining was very intense in the peripheral MD cells and became much fainter and more perinuclear in the central cells. The average number of Cox-2-positive central MD cells was 1.6 cells/MD in CLP rats, a significant increase from 0.6 cells/MD in sham-operated rats (not shown). These statistics were obtained from single-plane views of MD in each group rather than 3D reconstructions, hence the small number of cells in the statistics. The number of peripheral MD cells expressing Cox-2 also increased significantly with sepsis. These were included in the statistics with other Cox-2-positive cTAL cells. A video showing a reconstructed 3D MD can be found under supplemental material (Video 1; all supplemental material is available in the online version of this article at the journal website) and helps visualize the relationship between central and peripheral MD cells.

Outer medulla: sepsis increases Cox-2 expression in THP-positive mTAL. In sham rats, Cox-2 staining in the outer medulla was very faint in all segments (Fig. 6). After CLP, there was a significant increase in the intensity of mTAL Cox-2 staining.

Fig. 4. Immunofluorescence staining of cyclooxygenase (Cox)-2 in the renal cortex of sham and CLP rats. Shown are representative renal cortical sections from sham rats (A and C) and 24 h after CLP (B and D). Cox-2 immunofluorescence staining is shown in yellow (arrowheads). It is localized to discrete cTAL cells, which increase in both number and intensity after CLP (B, D, and E). The number of intense cells is reported per TAL pixels (E). THP staining is shown in red. In A and B, MD cells show no THP staining, and bright green fluorescence is FITC-phalloidin, used as a marker for proximal tubules (P), which show intense apical brush border staining. FITC-phalloidin also labels the actin cytoskeleton in other structures like glomeruli (G). Alternatively, proximal tubules were identified by their green autofluorescence (C and D). This autofluorescence is not apparent in A and B because the detectors had to be set at very low levels due to the bright FITC staining. Proximal and T- tubules showed minimal or no Cox-2 staining in either sham or CLP rats. * $P < 0.05$ CLP compared with sham.



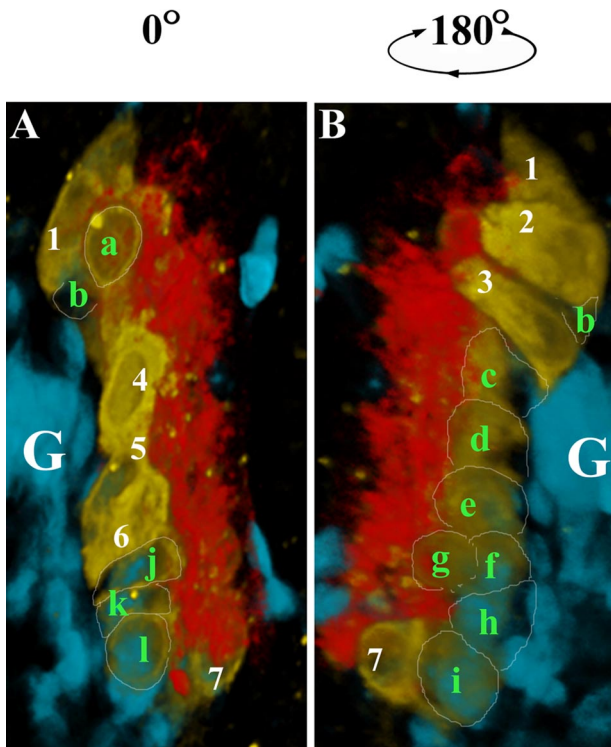


Fig. 5. Three-dimensional (3D) projection of a rat MD with Cox-2 staining of central and peripheral cells. The figure represents a 3D volume reconstruction of a MD from a CLP rat. The volume is projected into the plane and shown in 2 different angular rotations. Cox-2 fluorescence is shown in yellow. The MD band of cells is composed of peripheral and more central cells. Peripheral MD cells (labeled numerically) have intense cytoplasmic Cox-2 staining. More central MD cells (labeled alphabetically with hand-drawn contours) have fainter perinuclear staining. THP staining (absent from MD cells) is shown in red and labels opposing equiplanar cells to the MD. Glomerular cells adjacent to the MD are labeled G. All nuclei are stained blue with DAPI. See also supplemental material (Video 1).

This increase was cellular but also intensified at the apical border of tubules. In contrast to cTAL, Cox-2 staining in the mTAL is diffuse and linear along the tubules. Cox-2 fluorescence in THP-negative tubules (representing primarily CD) and proximal tubules (in the OSOM) did not change significantly after CLP (Fig. 6G).

Inner medulla: sepsis increases Cox-2 expression in inner medullary CD. Under sham conditions, Cox-2 staining was faint and limited primarily to CD (Fig. 7). After CLP, there was a significant increase in the intensity of CD Cox-2 staining that extended throughout the cell with apical accentuation. Cox-2 staining of structures labeled I in the figure (vessels, thin descending limbs and TAL as well as interstitial cells) did not increase after CLP.

Changes in Renal Cox-2 Expression With Sepsis in Wild-Type and *TLR4*^{-/-} Mutant Mice

To investigate the dependence of renal Cox-2 induction in sepsis on TLR4, we studied the effect of CLP on Cox-2 expression in wild-type (*TLR4*^{+/+}) and *TLR4*^{-/-} mice.

Cortex: sepsis-induced increase in Cox-2 is TLR4 dependent in cTAL and partially TLR4 dependent in proximal tubules. In *TLR4*^{+/+} mice, Cox-2 staining was very weak in the renal cortex of sham animals (Fig. 8). After CLP, there was a significant increase in Cox-2 staining in cTAL tubules. Unlike our findings in the rat, Cox-2 staining in mice cTAL was diffuse throughout all tubular cells rather than restricted to individual ones. Furthermore, mice proximal tubules also showed a significant increase in Cox-2 after CLP, a finding not observed in the rat. In *TLR4*^{-/-} mice, there was no significant increase in Cox-2 fluorescence after CLP in cTAL. Furthermore, while the increase in proximal tubular Cox-2 fluorescence remained significant, it was of a considerably smaller magnitude than that observed in *TLR4*^{+/+}

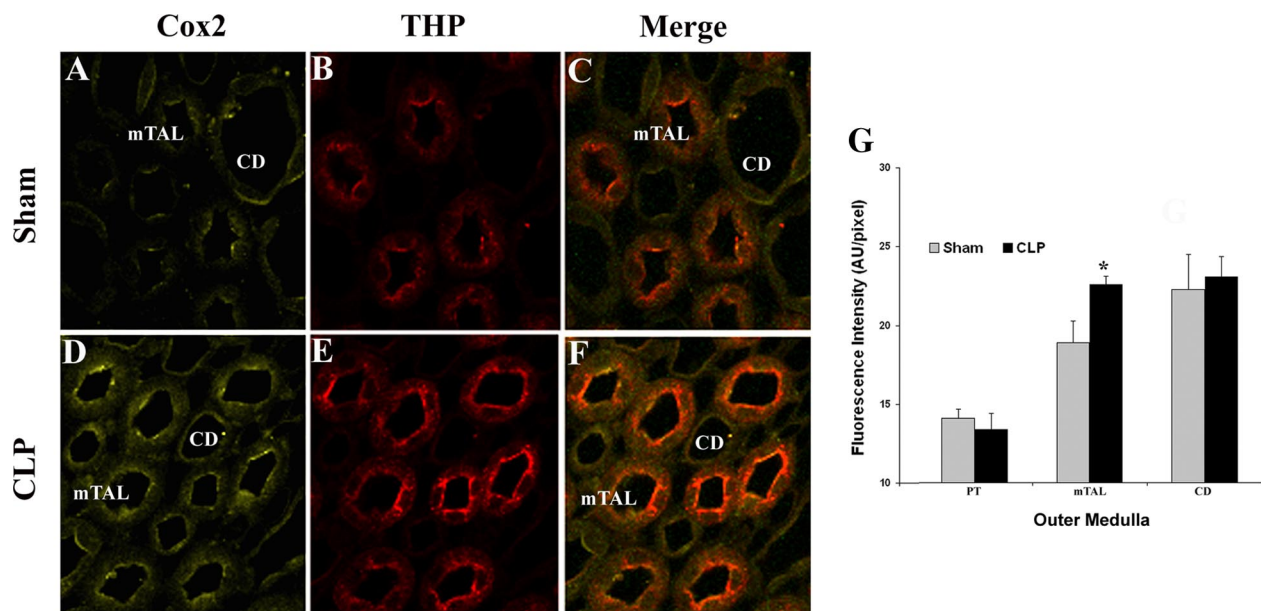
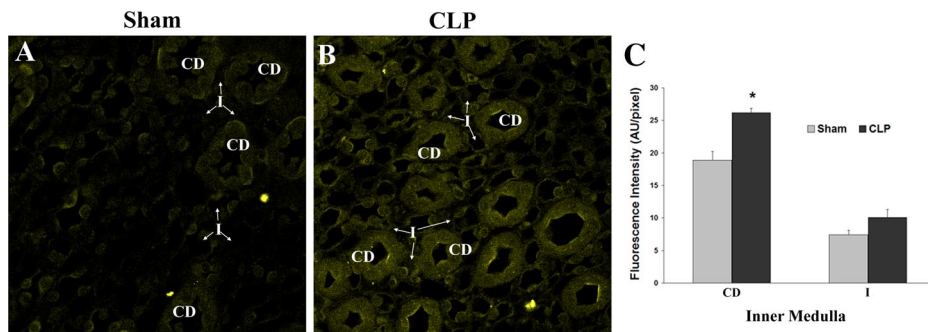


Fig. 6. Immunofluorescence staining of Cox-2 in the renal outer medulla of sham and CLP rats. Shown are representative sections from the inner stripe of the outer medulla (ISOM) of rats under sham conditions (A–C) and 24 h after CLP (D–F). Cox-2 immunofluorescence (A and D) is shown in yellow. THP fluorescence in mTAL segments is shown in red (B and E). C and F: merged yellow and red channels. THP-negative tubules represent primarily CD. The outer stripe of the outer medullary (OSOM; which contains proximal tubules in addition to mTAL and CD) showed changes in Cox-2 staining similar to the ISOM. G: quantitative changes in Cox-2 fluorescence in the major outer medullary tubules. * $P < 0.05$ CLP compared with sham.

Fig. 7. Immunofluorescence staining of Cox-2 in the renal inner medulla of sham and CLP rats. Shown are representative sections from the inner medulla of rats under sham conditions or 24 h after CLP. Cox-2 fluorescence is shown in yellow. CD are the most prominent tubular structures. Smaller structures (labeled I) in between CD are vessels, TAL, descending thin limbs, or interstitial cells. C: quantitation of changes in Cox-2 fluorescence. * $P < 0.05$ CLP compared with sham.



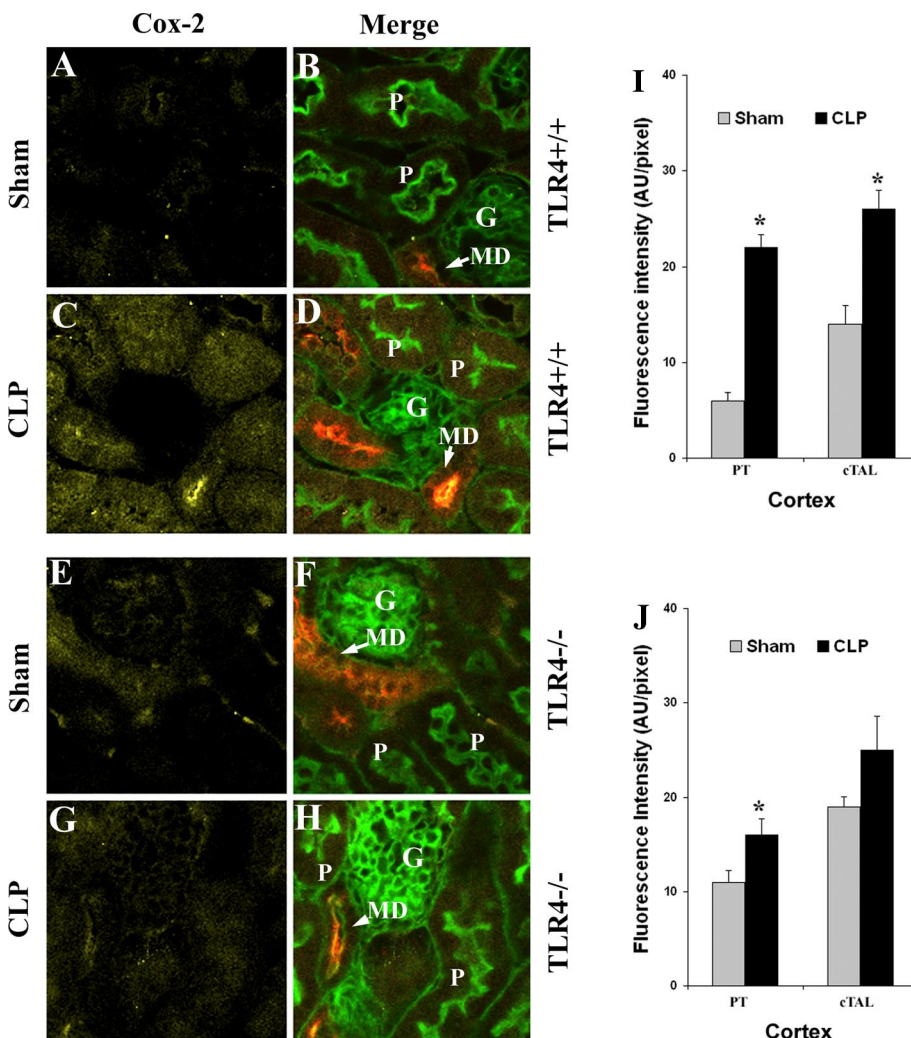
mice. In $TLR4^{+/+}$ MD cells, Cox-2 increased after CLP from 6 to 17 AU/pixel ($P < 0.05$). The changes in MD Cox-2 were not significant in mutant $TLR4^{-/-}$ mice. Unlike rat MD, mouse MD could not be resolved into central and peripheral cells.

Outer medulla: sepsis-induced increase in Cox-2 is TLR4 dependent in mTAL. In sham $TLR4^{+/+}$ mice, Cox-2 staining was faint but present in all tubules of the outer medulla, i.e., mTAL, CD, and even late proximal tubule segments of the outer stripe. However, the staining was most intense in CD (Fig. 9). After CLP, there was a significant increase in Cox-2

fluorescence only in mTAL. In CD, the average tubular Cox-2 fluorescence did not change with sepsis, but a prominent redistribution of the signal toward the apical border was noted. In contrast, $TLR4^{-/-}$ mutant mice did not show any increase in mTAL Cox-2 fluorescence after CLP. Like in the wild-type mouse, the total CD Cox-2 fluorescence was not increased after CLP. Rather, it only showed redistribution toward the apical border of the tubule.

Inner medulla: sepsis-induced Cox-2 in mouse inner medulla is not TLR4 dependent. In $TLR4^{+/+}$ mice, CLP induced a very significant increase in Cox-2 fluorescence of

Fig. 8. Immunofluorescence staining of Cox-2 in the renal cortex of sham and CLP mice. Representative sections from wild-type ($TLR4^{+/+}$) and mutant ($TLR4^{-/-}$) mice under sham condition or after CLP, $TLR4$ is Toll-like receptor 4 gene. Cox-2 fluorescence is shown in the yellow channel alone (A, C, E, and G) or merged with green FITC-phalloidin and red THP. Labels are similar to those used in the rat-related figures. I and J: quantitation of Cox-2 changes with CLP in wild-type and mutants. Note that, unlike in rats, Cox-2 fluorescence in mice cTAL is diffuse in the whole tubule rather than limited to few discrete cells. Also, in contrast to the rat findings, mice proximal tubules show a significant increase in Cox-2 fluorescence after CLP. * $P < 0.05$ CLP compared with sham.



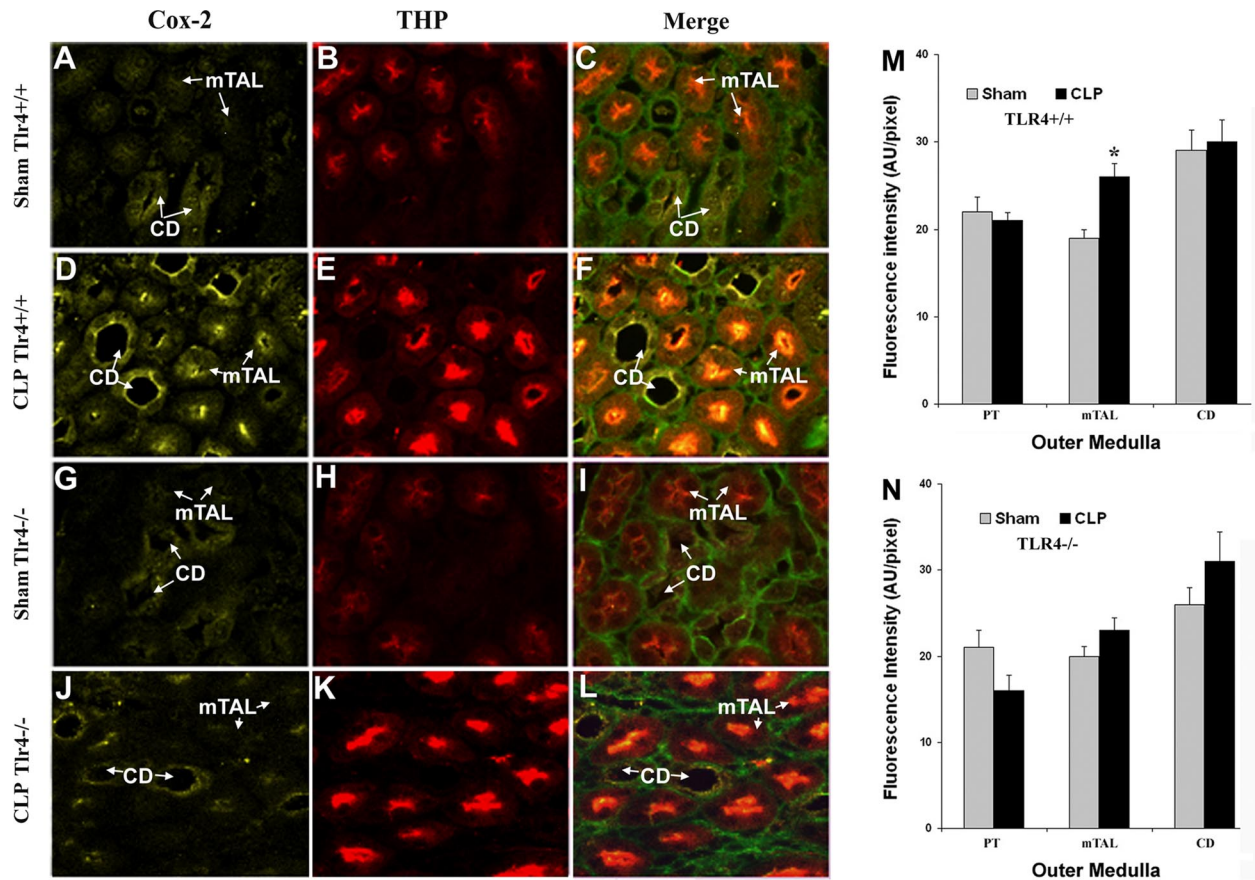


Fig. 9. Immunofluorescence staining of Cox-2 in the renal outer medulla of sham and CLP mice. Shown are representative sections from the ISOM of *TLR4*^{+/+} and *TLR4*^{-/-} mutant mice under sham conditions (A–F) or after CLP (G–L). Cox-2 channel (yellow) and THP channel (red) are shown separately then merged along with green FITC. M and N: quantitation of Cox-2 changes with sepsis in the outer medulla. Note that in the wild-type mouse, total cellular CD Cox-2 fluorescence did not increase after CLP. However, there was a prominent shift of the signal toward the apical border of CD tubules. The OSOM (which contains proximal tubules in addition to mTAL and CD) showed changes in Cox-2 staining similar to the ISOM in both mice strains. **P* < 0.05 CLP compared with sham.

inner medullary structures found in between CD. These structures (labeled I in Fig. 10) represent vessels, thin descending limbs and TAL as well as interstitial cells. This increase was not TLR4 dependent as it was also observed in

mutant *TLR4*^{-/-} mice. Both wild-type and mutant mice also showed Cox-2 fluorescence in inner medullary CD under sham conditions. This CD Cox-2 fluorescence was slightly decreased in both mice strains after CLP. This

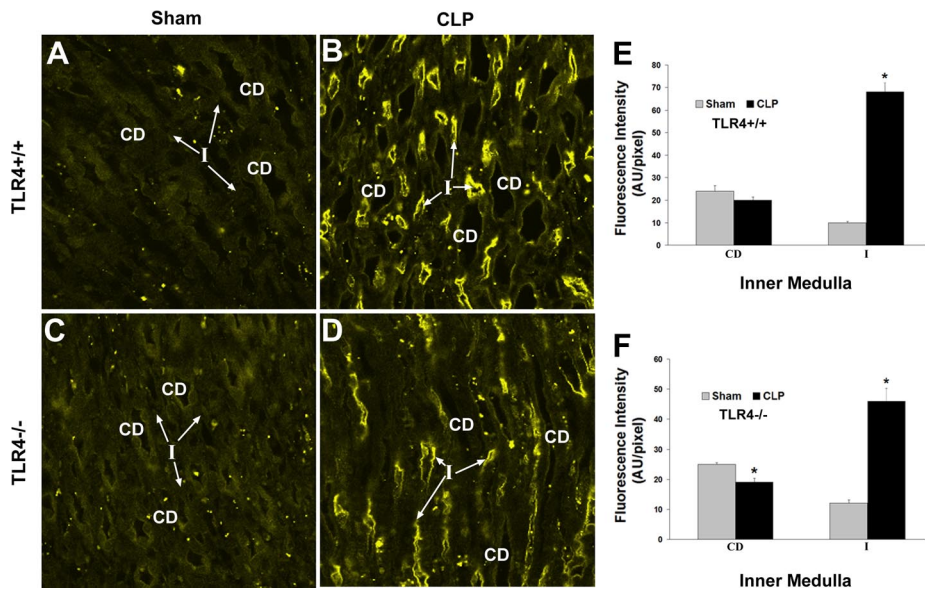


Fig. 10. Immunofluorescence staining of Cox-2 in the renal inner medulla of sham and CLP mice. Shown are representative sections from the inner medulla of *TLR4*^{+/+} and *TLR4*^{-/-} mutant mice under sham conditions or 24 h after CLP. Cox-2 fluorescence is shown in yellow. CD are the most prominent tubular structures. Smaller structures (labeled I) in between CD are vessels, TAL, and descending thin limbs or interstitial cells. E and F: quantitation of changes in Cox-2 fluorescence. **P* < 0.05 CLP compared with sham.

contrasted with the significant CLP-induced increase observed in rat inner medullary CD.

Juxtaglomerular Cell Renin is Absent in TLR4-Deficient Mice

Renin secretion in the cortex is partly regulated through Cox-2 produced in the cTAL/MD area (32). Since our results suggest that TLR4 is involved in Cox-2 regulation in these tubular segments, we examined the effect of TLR4 absence on renin expression (Fig. 11). In *TLR4*^{+/+} mice, renin staining was identified in granular cells adjacent to the MD and in the branching arteriolar tree. With sepsis, renin staining was still identified in the vascular tree but was not found in granular cells, possibly suggesting release of renin (data not shown). In sham mutant mice, we could not detect any renin staining in granular cells, although it was still present in branching arterioles. CLP did not alter the pattern of renin expression in these mutant mice.

DISCUSSION

In this study, we examined the effects of CLP, a physiologically relevant model of sepsis, on renal Cox-2 expression. We show that in both rats and mice, CLP induces significant increases in Cox-2 protein in various nephronal segments. We also show that TLR4 is necessary for CLP-induced Cox-2 expression only in cTAL and mTAL, tubules that express THP. Renal Cox-2 signaling is involved in many important regulatory functions under both physiological and pathophysiological conditions (15, 24, 26, 32). Therefore, the identification of

TLR4 as a major regulatory protein for renal Cox-2 expression can have profound implications in both health and disease.

In sham rat kidneys, Cox-2 expression was similar to what was reported previously by others (12, 16, 25, 34, 38). In contrast, the changes we report in our model of sepsis are only in partial agreement with previous literature. Of note is that other investigators relied primarily on LPS injection models (18, 40). These typically generate a cytokine profile drastically different from that seen with CLP (33). The data also depend on the time points investigated, the LPS dose, and the bacterial strain of origin. For example, 24 h after 2 mg/kg *Escherichia coli* LPS, Ichitani et al. (18) reported an increase in Cox-2 mRNA (in situ hybridization) in rat cortex, outer, and inner medulla. Conversely, using 4 mg/kg salmonella LPS, Yang et al. (40) found a significant increase in Cox-2 mRNA (RT-PCR) and protein (Western blotting) at 8 h only in the inner medulla of rats. Cox-2 expression in the cortex was not significantly altered. They further supported their findings by detecting CD14, a protein necessary for LPS signaling, only in medullary CD cells.

In our model of rat CLP, Cox-2 increased significantly in cTAL, mTAL, and inner medullary CD. These are all segments that strongly express TLR4. We have also previously reported strong expression of CD14 in the rat cortex (10). In addition, we note that the soluble form of CD14 increases in the blood with sepsis and is easily detectable in the urine (4). Thus both CD14 and TLR4 are available for signaling throughout most nephronal segments. Therefore, we were surprised at the lack of Cox-2 changes in proximal tubules. Indeed, these express CD14 and do take up LPS as we have previously shown in live animal studies (10). It is possible that rat proximal tubules lack some of the TLR4 signaling pathways leading to Cox-2 generation.

To our knowledge, there are no previous studies that specifically investigated renal Cox-2 in septic mice. There is even considerable controversy regarding Cox-2 expression in sham mice (5, 35). In our hands, Cox-2 expression under sham conditions was most prominent in the collecting ducts of the inner and outer medulla. After CLP, cortical PT, cTAL, and mTAL showed the greatest increases in Cox-2. Thus the findings in mice and rats differed in many significant ways. First, the expression of Cox-2 in mice cTAL was diffuse along the segment, in contrast to its presence in discrete cells in rat cTAL. Second, the increase in mice PT Cox-2 was not observed in the rat. Third, the increase in rat CD Cox-2 was absent in the mouse. Finally, mouse inner medullary interstitial areas showed a dramatic increase in CLP-induced Cox-2 staining that was not seen in the rat. These findings underscore major species-specific differences in renal Cox-2 expression in sepsis.

As to the TLR4 dependence of Cox-2 changes in the mouse kidney, we found that they were restricted mostly to THP-expressing cTAL and mTAL segments. It is remarkable that these are also the only segments where both mice and rats showed similar changes in Cox-2 expression. These segments also showed a significant increase in THP after CLP in both species. Therefore, it is possible that THP, recently shown to be a ligand of TLR4 on dendritic cells (31), is also involved in TLR4-mediated Cox-2 signaling in TAL segments of mice and rats. Indeed, we have previously colocalized TLR4 and THP in these nephronal segments (10). Furthermore, it was recently

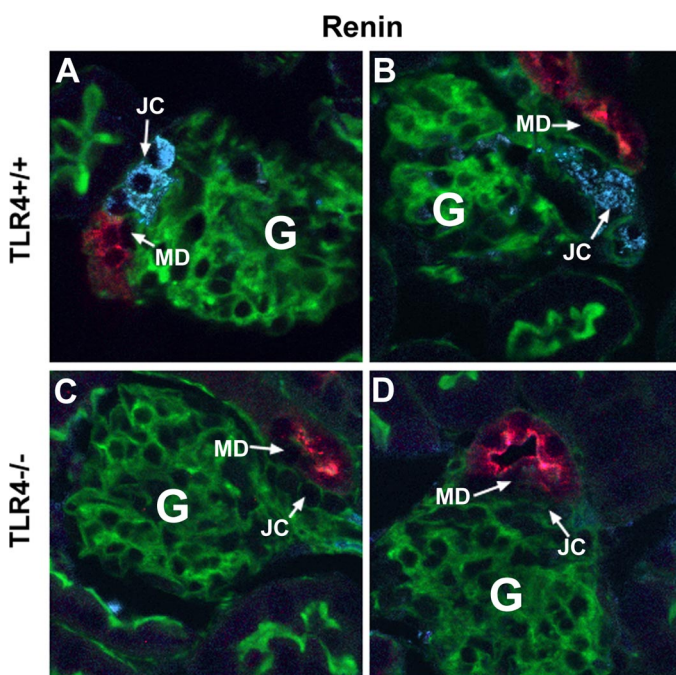


Fig. 11. Immunofluorescence staining of renin in the macula densa of *TLR4*^{+/+} and *TLR4*^{-/-} mutant mice. Shown are representative sections from the cortex of *TLR4*^{+/+} and *TLR4*^{-/-} mutant sham mice. In A and B, juxtaglomerular cells (JC) of *TLR4*^{+/+} mice contain renin (shown in blue). THP is shown in red. MD cells contain no THP and are adjacent to JC. In C and D, JC cells of mutant mice show no renin staining. Mutant mice did, however, show renin staining in arteriolar structures away from MD cells (not shown). Other labels are as described before.

shown that THP knockout mice have reduced renal Cox-2 expression (3). It is thus very tempting to speculate that this TLR4-dependent Cox-2 signaling is initiated in part by THP.

Our studies do not specifically address the role of systemic vs. local TLR4 in TAL Cox-2 expression. However, previous studies showed that LPS induces prostaglandins in primary cultures of rat mTAL cells, thus precluding other systemic influences (11, 13). Furthermore, the possible signaling role of THP in these tubules also suggests the involvement of local TLR4 in Cox-2 generation. Further experiments are needed to fully elucidate a direct effect of THP on renal cell TLR4 and its role in Cox-2 signaling.

The TLR4-independent changes in Cox-2 in other nephronal segments could be related to various local or systemic factors. For example, it is remarkable that the induction of Cox-2 in mouse inner medullary interstitium with sepsis is comparable to what is seen with other stimuli like dehydration (15). This effect was also TLR4 independent. Thus it is possible that our CLP model in the mouse does generate hemodynamic effects similar to dehydration that are sensed by inner medullary interstitial cells.

Cox-2 expression in the rat MD has been a subject of controversy. This stems in part from the inconsistent description of Cox-2-expressing cells in relation to the MD (18). Indeed, the region of the MD in rats harbors at least two populations of cells expressing Cox-2 (5). One type shows Cox-2 staining around the nuclear envelope and has been considered to represent the MD proper (5). The other population of cells shows diffuse and intense cytosolic Cox-2 staining. The location of these latter cells is not obvious from plane cross-sectional cuts and tends to vary with the angle of the cut. Our 3D volume reconstruction shows them as occupying a peripheral position surrounding, and in close contact with, proper MD cells. The contribution of each cell type to functions generically attributed to the MD is unknown. Of note is that these peripheral MD cells had morphological traits comparable to the other dispersed Cox-2-positive cTAL cells and might just be part of this disseminated Cox-2-expressing system.

In contrast to the rat, mice cTAL and MD cells showed diffuse Cox-2 staining that was not localized to specific cells. Like in cTAL, the increase in mouse MD Cox-2 staining after CLP was TLR4 dependent. We also note that THP is not expressed in MD cells of mice and rats. However, cells opposing the MD in the same cross-sectional area have abundant THP (Figs. 2 and 5). Thus it is possible that THP secreted from these cells has access to the MD and plays a role in Cox-2 signaling.

Finally, a major finding in this paper was the baseline absence of renin in juxtaglomerular cells of the TLR4 knockout mouse. This was specific to juxtaglomerular cells as renin was easily detected in other arteriolar segments. Because activation of the renin-angiotensin axis has been implicated in vascular reactivity and kidney injury in sepsis (36), the absence of juxtaglomerular cell renin in TLR4 knockout mice might explain the milder renal injury in these mice after CLP (unpublished observations). Furthermore, our findings relating TLR4 to Cox-2 and renin could have significant implications that extend well beyond the realm of sepsis. Indeed, with endogenous ligands like THP, TLR4 could be involved in the regulation of functions as diverse as ion transport, renal blood flow, systemic hemodynamics, and hypertension.

In summary, we have presented the first systematic characterization of renal Cox-2 expression in rats and mice in a physiologically relevant model of sepsis. We further showed the importance of TLR4 in sepsis-induced cTAL and mTAL Cox-2 expression. TLR4 is also essential for baseline renin expression in juxtaglomerular cells. Finally, indirect evidence suggests a role for THP in TLR4-mediated Cox-2 signaling. Further studies are needed to establish a firm and direct link among THP, TLR4, and Cox-2 in the kidney.

GRANTS

This work was supported by National Institute of Diabetes and Digestive and Kidney Diseases Grant 1R01-DK-60495-01A1 (P. C. Dagher), a Paul Teschan research fund award (P. C. Dagher), and a National Kidney Foundation-Indiana grant (T. M. El-Achkar).

REFERENCES

1. Akira S, Takeda K. Toll-like receptor signalling. *Nat Rev Immunol* 4: 499–511, 2004.
2. Akira S, Uematsu S, Takeuchi O. Pathogen recognition and innate immunity. *Cell* 124: 783–801, 2006.
3. Bachmann S, Mutig K, Bates J, Welker P, Geist B, Gross V, Luft FC, Alenina N, Bader M, Thiele BJ, Prasad K, Raffi HS, Kumar S. Renal effects of Tamm-Horsfall protein (uromodulin) deficiency in mice. *Am J Physiol Renal Physiol* 288: F559–F567, 2005.
4. Bussolati B, David S, Cambi V, Tobias PS, Camussi G. Urinary soluble CD14 mediates human proximal tubular epithelial cell injury induced by LPS. *Int J Mol Med* 10: 441–449, 2002.
5. Campean V, Theilig F, Paliege A, Breyer M, Bachmann S. Key enzymes for renal prostaglandin synthesis: site-specific expression in rodent kidney (rat, mouse). *Am J Physiol Renal Physiol* 285: F19–F32, 2003.
6. Cunningham PN, Wang Y, Guo R, He G, Quigg RJ. Role of Toll-like receptor 4 in endotoxin-induced acute renal failure. *J Immunol* 172: 2629–2635, 2004.
7. Dear JW, Yasuda H, Hu X, Hieny S, Yuen PS, Hewitt SM, Sher A, Star RA. Sepsis-induced organ failure is mediated by different pathways in the kidney and liver: acute renal failure is dependent on MyD88 but not renal cell apoptosis. *Kidney Int* 69: 832–836, 2006.
8. Ejima K, Layne MD, Carvajal IM, Kritek PA, Baron RM, Chen YH, Vom Saal J, Levy BD, Yet SF, Perrella MA. Cyclooxygenase-2-deficient mice are resistant to endotoxin-induced inflammation and death. *FASEB J* 17: 1325–1327, 2003.
9. El-Achkar TM, Dagher PC. Renal Toll-like receptors: recent advances and implications for disease. *Nat Clin Pract Nephrol* 2: 568–581, 2006.
10. El-Achkar TM, Huang X, Plotkin Z, Sandoval RM, Rhodes GJ, Dagher PC. Sepsis induces changes in the expression and distribution of Toll-like receptor 4 in the rat kidney. *Am J Physiol Renal Physiol* 290: F1034–F1043, 2006.
11. Escalante BA, Ferreri NR, Dunn CE, McGiff JC. Cytokines affect ion transport in primary cultured thick ascending limb of Henle's loop cells. *Am J Physiol Cell Physiol* 266: C1568–C1576, 1994.
12. Ferreri NR, An SJ, McGiff JC. Cyclooxygenase-2 expression and function in the medullary thick ascending limb. *Am J Physiol Renal Physiol* 277: F360–F368, 1999.
13. Ferreri NR, McGiff JC, Vio CP, Carroll MA. TNF α regulates renal COX-2 in the rat thick ascending limb (TAL). *Thromb Res* 110: 277–280, 2003.
14. Fu JY, Masferrer JL, Seibert K, Raz A, Needleman P. The induction and suppression of prostaglandin H₂ synthase (cyclooxygenase) in human monocytes. *J Biol Chem* 265: 16737–16740, 1990.
15. Hao CM, Yull F, Blackwell T, Komhoff M, Davis LS, Breyer MD. Dehydration activates an NF- κ B-driven, COX2-dependent survival mechanism in renal medullary interstitial cells. *J Clin Invest* 106: 973–982, 2000.
16. Harris RC, McKanna JA, Akai Y, Jacobson HR, Dubois RN, Breyer MD. Cyclooxygenase-2 is associated with the macula densa of rat kidney and increases with salt restriction. *J Clin Invest* 94: 2504–2510, 1994.
17. Heyman SN, Lieberthal W, Rogiers P, Bonventre JV. Animal models of acute tubular necrosis. *Curr Opin Crit Care* 8: 526–534, 2002.

18. Ichitani Y, Holmberg K, Maunsbach AB, Haeggstrom JZ, Samuelsson B, De Witt D, Hokfelt T. Cyclooxygenase-1 and cyclooxygenase-2 expression in rat kidney and adrenal gland after stimulation with systemic lipopolysaccharide: in situ hybridization and immunocytochemical studies. *Cell Tissue Res* 303: 235–252, 2001.
19. Kelly KJ, Plotkin Z, Dagher PC. Guanosine supplementation reduces apoptosis and protects renal function in the setting of ischemic injury. *J Clin Invest* 108: 1291–1298, 2001.
20. Kelly KJ, Sandoval RM, Dunn KW, Molitoris BA, Dagher PC. A novel method to determine specificity and sensitivity of the TUNEL reaction in the quantitation of apoptosis. *Am J Physiol Cell Physiol* 284: C1309–C1318, 2003.
21. Kelly KJ, Sutton TA, Weathered N, Ray N, Caldwell EJ, Plotkin Z, Dagher PC. Minocycline inhibits apoptosis and inflammation in a rat model of ischemic renal injury. *Am J Physiol Renal Physiol* 287: F760–F766, 2004.
22. Leemans JC, Stokman G, Claessen N, Rouschop KM, Teske GJ, Kirschning CJ, Akira S, van der Poll T, Weening JJ, Florquin S. Renal-associated TLR2 mediates ischemia/reperfusion injury in the kidney. *J Clin Invest* 115: 2894–2903, 2005.
23. Miyaji T, Hu X, Yuen PS, Muramatsu Y, Iyer S, Hewitt SM, Star RA. Ethyl pyruvate decreases sepsis-induced acute renal failure and multiple organ damage in aged mice. *Kidney Int* 64: 1620–1631, 2003.
24. Nasrallah R, Hebert RL. Prostacyclin signaling in the kidney: implications for health and disease. *Am J Physiol Renal Physiol* 289: F235–F246, 2005.
25. Nasrallah R, Landry A, Singh S, Sklepowicz M, Hebert RL. Increased expression of cyclooxygenase-1 and -2 in the diabetic rat renal medulla. *Am J Physiol Renal Physiol* 285: F1068–F1077, 2003.
26. Norregaard R, Jensen BL, Li C, Wang W, Knepper MA, Nielsen S, Frokiaer J. COX-2 inhibition prevents downregulation of key renal water and sodium transport proteins in response to bilateral ureteral obstruction. *Am J Physiol Renal Physiol* 289: F322–F333, 2005.
27. Peti-Peterdi J, Komlosi P, Fuson AL, Guan Y, Schneider A, Qi Z, Redha R, Rosivall L, Breyer MD, Bell PD. Luminal NaCl delivery regulates basolateral PGE₂ release from macula densa cells. *J Clin Invest* 112: 76–82, 2003.
28. Phillips CL, Arend LJ, Filson AJ, Kojetin DJ, Clendenon JL, Fang S, Dunn KW. Three-dimensional imaging of embryonic mouse kidney by two-photon microscopy. *Am J Pathol* 158: 49–55, 2001.
29. Riedemann NC, Guo RF, Ward PA. The enigma of sepsis. *J Clin Invest* 112: 460–467, 2003.
30. Rifkin IR, Leadbetter EA, Busconi L, Viglianti G, Marshak-Rothstein A. Toll-like receptors, endogenous ligands, and systemic autoimmune disease. *Immunol Rev* 204: 27–42, 2005.
31. Saemann MD, Weichhart T, Zeyda M, Staffler G, Schunn M, Stuhlmeier KM, Sobanov Y, Stulnig TM, Akira S, von Gabain A, von Ahsen U, Horl WH, Zlabinger GJ. Tamm-Horsfall glycoprotein links innate immune cell activation with adaptive immunity via a Toll-like receptor-4-dependent mechanism. *J Clin Invest* 115: 468–475, 2005.
32. Schnermann WJ. Homer Smith Award lecture. The juxtaglomerular apparatus: from anatomical peculiarity to physiological relevance. *J Am Soc Nephrol* 14: 1681–1694, 2003.
33. Villa P, Sartor G, Angelini M, Sironi M, Conni M, Gnocchi P, Isetta AM, Grau G, Buurman W, van Tits LJ, Ghezzi P. Pattern of cytokines and pharmacomodulation in sepsis induced by cecal ligation and puncture compared with that induced by endotoxin. *Clin Diagn Lab Immunol* 2: 549–553, 1995.
34. Vio CP, Cespedes C, Gallardo P, Masferrer JL. Renal identification of cyclooxygenase-2 in a subset of thick ascending limb cells. *Hypertension* 30: 687–692, 1997.
35. Wagner C, Vitzthum H, Castrop H, Schumacher K, Bucher M, Albertin S, Coffman TM, Arendshorst WJ, Kurtz A. Differential regulation of renin and Cox-2 expression in the renal cortex of C57Bl/6 mice. *Pflügers Arch* 447: 214–222, 2003.
36. Wang W, Falk SA, Jittikanont S, Gengaro PE, Edelstein CL, Schrier RW. Protective effect of renal denervation on normotensive endotoxemia-induced acute renal failure in mice. *Am J Physiol Renal Physiol* 283: F583–F587, 2002.
37. Wichterman KA, Baue AE, Chaudry IH. Sepsis and septic shock—a review of laboratory models and a proposal. *J Surg Res* 29: 189–201, 1980.
38. Yang T, Schnermann JB, Briggs JP. Regulation of cyclooxygenase-2 expression in renal medulla by tonicity in vivo and in vitro. *Am J Physiol Renal Physiol* 277: F1–F9, 1999.
39. Yang T, Singh I, Pham H, Sun D, Smart A, Schnermann JB, Briggs JP. Regulation of cyclooxygenase expression in the kidney by dietary salt intake. *Am J Physiol Renal Physiol* 274: F481–F489, 1998.
40. Yang T, Sun D, Huang YG, Smart A, Briggs JP, Schnermann JB. Differential regulation of COX-2 expression in the kidney by lipopolysaccharide: role of CD14. *Am J Physiol Renal Physiol* 277: F10–F16, 1999.
41. Zager RA, Johnson AC, Lund S, Randolph-Habecker J. Toll-like receptor (TLR4) shedding and depletion: acute proximal tubular cell responses to hypoxic and toxic injury. *Am J Physiol Renal Physiol* 292: F304–F312, 2007.